Efficient entry of cell-penetrating peptide nona-arginine into adherent cells involves a transient increase in intracellular calcium

Kamran Melikov*[1], Ann Hara*, Kwabena Yamoah*, Elena Zaitseva*, Eugene Zaitsev* and Leonid V. Chernomordik*

*Section on Membrane Biology, Program of Physical Biology, Eunice Kennedy Shriver National Institute of Child Health and Human Development, National Institutes of Health, Building 10/Room 10D05, 10 Center Drive, Bethesda, MD 20892-1855, U.S.A.

Understanding the mechanism of entry of cationic peptides such as nona-arginine (R_9) into cells remains an important challenge to their use as efficient drug-delivery vehicles. At nanomolar to low micromolar R_9 concentrations and at physiological temperature, peptide entry involves endocytosis. In contrast, at a concentration $\geqslant 10$ μM, R_9 induces a very effective non-endocytic entry pathway specific for cationic peptides. We found that a similar entry pathway is induced at 1–2 μM concentrations of R_9 if peptide application is accompanied by a rapid temperature drop to 15 °C. Both at physiological and at sub-physiological temperatures, this entry mechanism was inhibited by depletion of the intracellular ATP pool. Intriguingly, we found that R_9 at 10–20 μM and 37 °C induces repetitive spikes in intracellular Ca^{2+} concentration. This Ca^{2+} signalling correlated with the efficiency of the peptide entry. Pre-loading cells with the Ca^{2+} chelator BAPTA (1,2-bis(o-aminophenoxy)ethane-N,N,N′,N′-tetraacetic acid) inhibited both Ca^{2+} spikes and peptide entry, suggesting that an increase in intracellular Ca^{2+} precedes and is required for peptide entry. One of the hallmarks of Ca^{2+} signalling is a transient cell-surface exposure of phosphatidylserine (PS), a lipid normally residing only in the inner leaflet of the plasma membrane. Blocking the accessible PS with the PS-binding domain of lactadherin strongly inhibited non-endocytic R_9 entry, suggesting the importance of PS externalization in this process. To conclude, we uncovered a novel mechanistic link between calcium signalling and entry of cationic peptides. This finding will enhance our understanding of the properties of plasma membrane and guide development of future drug-delivery vehicles.

Key words: calcium imaging, calcium intracellular release, cell-penetrating peptide (CPP), microscopy, phosphatidylserine, transient receptor potential channels (TRP channels).

INTRODUCTION

Cell-penetrating peptides (CPPs) are a promising vehicle for delivery of macromolecular drugs. To date, CPPs have been used to deliver *in vitro* and *in vivo* a wide variety of different macromolecules including potentially therapeutic proteins, nucleic acids and bioactive peptides [1–3]. Despite significant progress in the identification and design of new CPPs, understanding of the mechanism of CPP entry into cell cytosol and nucleus is lacking. This is especially true in the case of highly cationic arginine-rich CPPs, such as TAT peptide and oligo-arginines of various lengths, for which cell membranes are expected to present a non-permeable barrier.

Arginine-rich CPPs added to cells at nanomolar to low micromolar concentrations at physiological temperature enter cells through various endocytic pathways [1,4–7]. Delivery of functionally active cargo molecules to their targets in cytosol and nucleus indicates that some fraction of CPP–cargo conjugate eventually escapes from endosomes. It has been suggested that endosome acidification [8,9] and/or changes in lipid composition of endosomes upon maturation [10,11] play an important role in CPP escape. However the efficiency of CPP release from endosomes is low, with most of the internalized peptide and cargo remaining trapped within endosomal compartments, as evidenced by the predominantly vesicular distribution of fluorescence-tagged peptide and a significant enhancement of delivery into the cytosol by endosome-destabilizing reagents [12,13]. In contrast, at concentrations $\geqslant 10$ μM at physiological temperature, arginine-rich CPPs have been shown to efficiently enter into the cytosol and nucleus through a pathway that apparently bypasses endocytosis [14–20]. The mechanism of this entry is the subject of considerable debate, with different groups suggesting involvement of dense CPP aggregates [15], CPP-induced transient plasma membrane deformations [19] and acid sphingomyelinase-dependent ceramide formation [20].

In the present paper, we report that a rapid (within a few seconds that are required for the buffer exchange) temperature decrease from 37 °C to 15 °C induces efficient entry of arginine-rich CPP nona-arginine (R_9) into adherent cells after 15–40 min of incubation in the presence of low peptide concentrations (2–5 μM). This temperature-drop-induced entry (TDE) shares a number of similarities with the high-peptide-concentration-induced entry (HCE) mechanism. In particular, both pathways are inhibited by depletion of intracellular ATP and require a transient increase in intracellular calcium levels, indicating that TDE and HCE depend on cell metabolism and intracellular signalling. Both entry of extracellular calcium and release of calcium from intracellular stores are required for TDE and HCE. Inhibition of peptide entry by phosphatidylserine (PS)-binding C2 domain of lactadherin (LactC2) [21,22] indicates that cell-surface exposure of the anionic lipid PS, one of the known manifestations of intracellular calcium rise [23,24], plays a role in the entry mechanism. Like HCE, TDE is restricted to free peptide and low-molecular-mass cargo. Our data indicate that interactions of arginine-rich CPPs with cells activate intracellular signalling cascades that result in significant

Abbreviations: CPP, cell-penetrating peptide; HCE, high-peptide-concentration-induced entry; LactC2, C2 domain of lactadherin; PS, phosphatidylserine; R_9, nona-arginine; SERCA, sarcoplasmic/endoplasmic reticulum Ca^{2-}-ATPase; TDE, temperature-drop-induced entry.

[1] To whom correspondence should be addressed (email melikovk@mail.nih.gov).

changes in plasma membrane permeability for highly cationic peptides.

EXPERIMENTAL

Chemicals

R_9-TAMRA (carboxytetramethylrhodamine), R_9C(PEG2000)-TAMRA, R_9(lysozyme)-TAMRA and R_9(BSA)-TAMRA conjugates were custom-synthesized by GenScript. PEG2000 was conjugated to cysteine, BSA and lysozyme were conjugated to the C-terminus of the R_9 peptide and TAMRA was conjugated to the N-terminus. R_9-HiLyte was custom-synthesized by AnaSpec. Imipramine hydrochloride, nortriptyline hydrochloride, $LaCl_3$, chlorpromazine hydrochloride, flufenamic acid, HC030013, AP18 and EGTA were purchased from Sigma. Thapsigargin was from Cayman Chemicals, Ruthenium Red was from EMD Biosciences and AMTB hydrochloride was from Tocris Bioscience. BAPTA/AM was purchased from Invitrogen. Calcium-sensitive fluorescent dye (Cal-520 AM) was purchased from AAT Bioquest.

CPP internalization experiments and drug treatments

HeLa, IC-21, CV-1 and CHO-K1 cells were cultured in DMEM (Dulbecco's modified eagle medium) (Invitrogen) supplemented with 10 % FBS (Clontech), 2 mM glutamine (Invitrogen) and antibiotic/antimycotic mixture (Invitrogen) at 37 °C and 5 % CO_2. For experiments, ∼30 000 cells were seeded onto 35-mm glass-bottomed culture dishes (MatTek) and cultured overnight. Unless stated otherwise, cells were incubated with the peptide and drugs in HEPES-buffered saline containing 20 mM HEPES (4-(2-hydroxyethyl)-1-piperazineethanesulfonic acid)/NaOH (pH 7.4), 137 mM NaCI, 2.7 mM KCl, 0.32 mM Na_2HPO_4, 1.3 mM $CaCl_2$, 0.8 mM $MgSO_4$ and 25 mM D-glucose (HMEM). Before experiments, cells were washed twice with HMEM for 15 min each time at 37 °C. During the second wash, cell nuclei were labelled with membrane-permeant DNA dye Hoechst 33342 (1 μg/ml final concentration; Invitrogen). To start incubation with the peptide, 37 °C buffer was rapidly replaced with buffer at the desired temperature (4 °C, 15 °C, 25 °C or 37 °C) containing 2 μM R_9-TAMRA together with the drugs being tested. After incubation, cells were washed three times with HMEM and promptly imaged at room temperature without fixation. Membrane-impermeant dye SYTOX Green (1 μM final concentration; Invitrogen) was added after the final wash to label cells with impaired plasma membrane. In some experiments, SYTOX Green was present during incubation with the peptide. For ATP depletion, cells were pre-incubated with 10 mM NaN_3 and 10 mM 2-deoxy-D-glucose for 30 min at 37 °C and peptide-containing buffer was supplemented with 10 mM NaN_3 and 10 mM 2-deoxy-D-glucose. To buffer intracellular calcium, we loaded cells with the calcium chelator BAPTA by incubating them with 20 μM BAPTA/AM for 30 min at 37 °C. For treatment with imipramine (10 μM), nortriptyline (10 μM) or chlorpromazine (10 μg/ml) we incubated cells with drugs for 30 min at 37 °C and drugs were also present during incubation with R_9-TAMRA. The cation channel inhibitors HC030031 (2-(1,3-Dimethyl-2,6-dioxo-1,2,3,6-tetrahydro-7H-purin-7-yl)-N-(4-isopropylphenyl)acetamide) (1–100 μM), AP18 (1–100 μM), AMTB (5–100 μM), La^{3+} (100 μM) and Ruthenium Red (100 μM) were added during incubation with the peptide without pre-incubation. Thapsigargin, an inhibitor of the sarcoplasmic/endoplasmic reticulum Ca^{2+}-ATPases (SERCAs), was used in two different ways: (i) 200 nM drug was added simultaneously with the peptide to induce acute release of calcium from endoplasmic reticulum; and (ii) a 30-min incubation with 2 μM thapsigargin at 37 °C before peptide addition was used to deplete calcium from endoplasmic reticulum stores. To test the role of extracellular calcium in peptide entry, we applied peptide in calcium-free buffer containing 1 mM EGTA. LactC2 was expressed and purified according to a previously described protocol [25]. LactC2 plasmid was a gift from Dr Gary B. Gilbert. To block cell-surface PS, LactC2 was added simultaneously with the peptide at a 100 μg/ml concentration.

Image acquisition and analysis

Images were acquired with an inverted fluorescence microscope (AxioObserver D1; Zeiss) equipped with a 20 × 0.8 numerical aperture (NA) Plan-Apochromat objective (Zeiss), LUDL filter wheels on both the epifluorescence illumination port and the image acquisition side port, CoolLed pE-2 LED illuminator (380, 490, 550 and 635 nm) and an Ixon 885 EMCCD camera (Andor). Microscope, lasers and camera were controlled with Micro-Manager 1.4.13. Fluorescence channels were collected sequentially through a quad-band dichroic (405/488/561/640; Semrock). To follow changes in intracellular calcium, cells were loaded with calcium sensitive dye Cal-520 AM (2 μM) for 30 min at 37 °C. This was followed by three washes and a 30-min incubation in dye-free buffer at room temperature (25 °C) to remove unconverted dye. After three more washes, cells were transferred into a DH-35iL microscope stage culture dish incubator (Warner Instruments) maintained at 37 °C. Cells were allowed to equilibrate for ∼5 min before the start of the imaging. We performed image analysis using an ImageJ script developed in-house. We also confirmed that loading cells with BAPTA/AM inhibits increase in intracellular calcium in response to a 10 μM peptide concentration (Supplementary Video S1). Time-lapse imaging experiments were performed only at 37 °C because of technical problems associated with refocusing required after the rapid change of temperature that was used to induce TDE.

RESULTS

Rapid temperature drop induces efficient entry of R_9 into the cytosol and nucleus

Low temperature slows down most metabolic processes and significantly inhibits endocytosis, the main pathway of peptide entry at low concentrations (<10 μM) of arginine-rich CPPs at physiological temperature [1,4–7]. While investigating energy-dependence of CPP entry into the cell, to our surprise, upon rapid transfer of HeLa cells into cold buffer (15 °C) containing 2 μM R_9-TAMRA, we observed many cells with strong R_9-TAMRA labelling of the cytosol and nucleus (Figure 1A). However, there was practically no entry of the peptide into other cells in the same dish (Figure 1A). As expected, endocytosis of CPP was significantly inhibited at 15 °C (note the absence of vesicular staining at 15 °C in the insets). Peptide entry was not due to a general loss of the barrier function of plasma membrane, as evidenced by a low fraction of cells (generally <0.1 %) labelled with the membrane-impermeant DNA dye SYTOX Green added either simultaneously with the peptide or at the end of the incubation period (results not shown). TDE was not limited to HeLa cells and was also observed in IC-21 cells (Supplementary Figure S1), CHO-K1 and CV-1 cells (results not shown). We also observed TDE of R_9-HiLyte–nona-arginine peptide labelled with

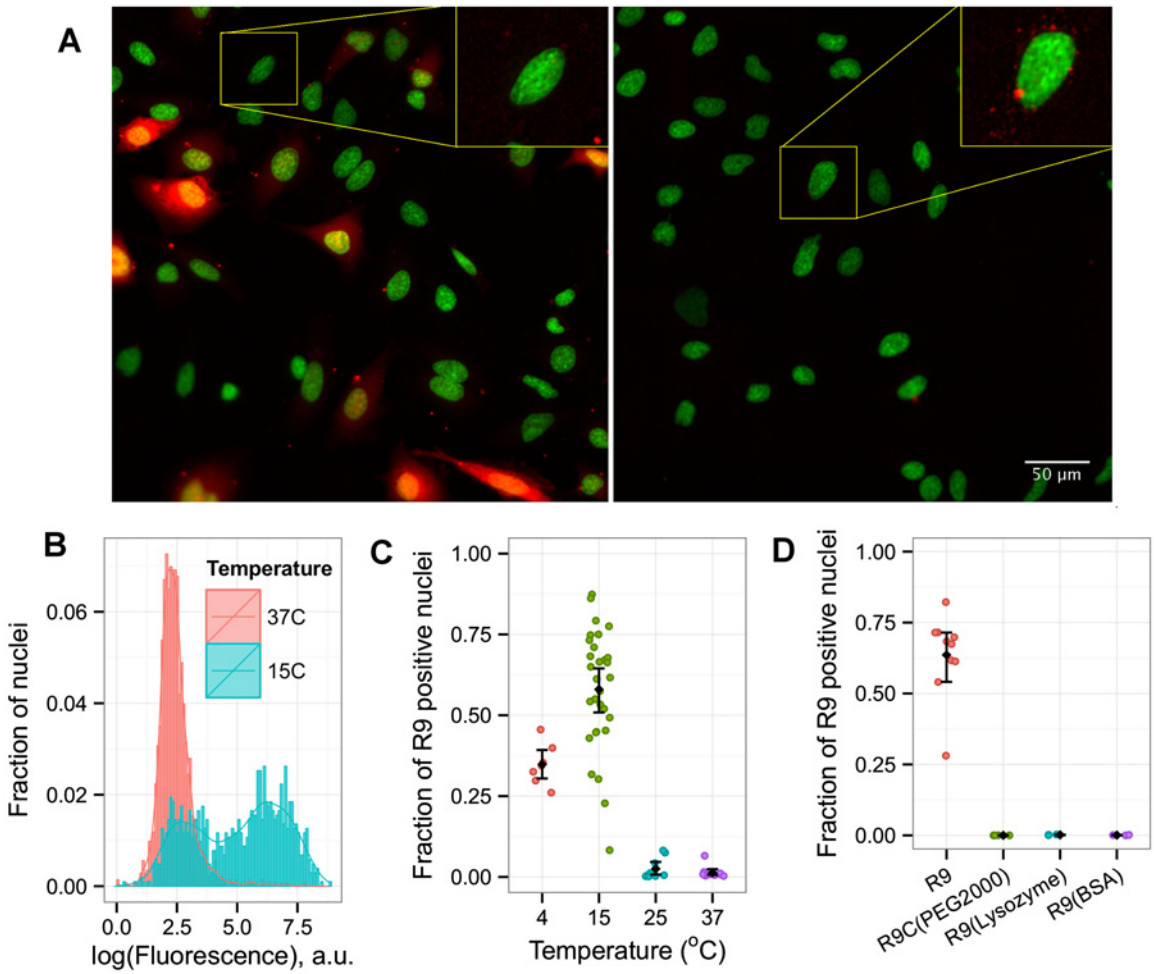

Figure 1 A temperature drop delivers R_9-TAMRA but not its high-molecular-mass conjugates into the cytosol and nucleus of HeLa cells

(**A**) Intracellular distribution of R_9-TAMRA (shown in red) after HeLa cells incubated at 37 °C were rapidly transferred into 15 °C (left panel) or 37 °C (right panel) buffer containing 2 μM peptide and incubated at the corresponding temperature for 15 min before washing and imaging. Cell nuclei were labelled with membrane-permeant DNA dye Hoechst 33342 (shown in green). Insets show ×2 magnification of an area within a yellow box with ×10-amplified fluorescence signal. (**B**) Frequency distribution of average per pixel R_9-TAMRA fluorescence of individual cell nuclei after a 15-min incubation with 2 μM peptide at 37 °C (red) or 15 °C (blue). (**C**) Dependence of fraction of cell nuclei with high fluorescence (R_9-positive nuclei) on the temperature of an incubation buffer. Cells were incubated with 2 μM peptide for 40 min before washing and imaging. (**D**) Fraction of R_9-positive nuclei after addition of 2 μM R_9-TAMRA, R_9C(PEG2000)-TAMRA (4 kDa), R_9(lysozyme)-TAMRA (16 kDa) or R_9(BSA)-TAMRA (66 kDa). Cells were incubated for 30 min at 15 °C before washing and imaging. Results of all individual experiments are shown as dots. Means for experiments together with 95 % confidence intervals are denoted by points with error bars.

another fluorescent dye (Supplementary Figure S2). Since cytosol and nucleus labelling were always correlated, we quantified non-endocytic R_9-TAMRA entry as an average per pixel fluorescence within cell nuclei. This approach allowed us to develop a simple automated quantification protocol and reduced the influence of endocytosis on our measurements. Distribution of fluorescence intensities in individual nuclei after rapid decrease in the buffer temperature to 15 °C was bimodal, with nuclei in the second peak significantly (>50-fold) brighter than nuclei of cells treated at 37 °C (Figure 1B). In contrast, the distribution observed after a 15-min incubation with 2 μM R_9-TAMRA at 37 °C was unimodal (Figure 1B). The fraction of cells demonstrating bright nuclear fluorescence was maximal (0.58 ± 0.071; mean ± 95 % confidence interval) when cells were incubated with the peptide at 15 °C (Figure 1C), with a significant but smaller fraction of nuclei positive for R_9-TAMRA at 4 °C (0.33 ± 0.065) and very few cells with nuclear staining at 25 °C (0.01 ± 0.016) and 37 °C (0.03 ± 0.082).

R_9 entry pathway opened by the temperature drop is transient

We observed R_9-TAMRA labelling of cell nuclei only when we replaced 37 °C buffer with 15 °C buffer already containing the peptide, i.e. R_9-TAMRA was present during rapid temperature change (Figure 2A). Pre-incubation of cells in the cold buffer before CPP addition for as little as 5 min strongly decreased the fraction of cells with a fluorescence-labelled nucleus (Figure 2A). A fast inactivation of the TDE pathway can also explain rapid levelling of the fraction of cells with R_9-TAMRA-labelled nuclei within 15 min of peptide addition (Figure 2B).

TDE is limited to fluorescent-dye-labelled peptide

As mentioned above, the rapid temperature drop increases plasma membrane permeability for R_9-TAMRA only in a fraction of cells. Similarly, heterogeneous labelling of cells with the peptide efficiently entering only a fraction of cells has been reported

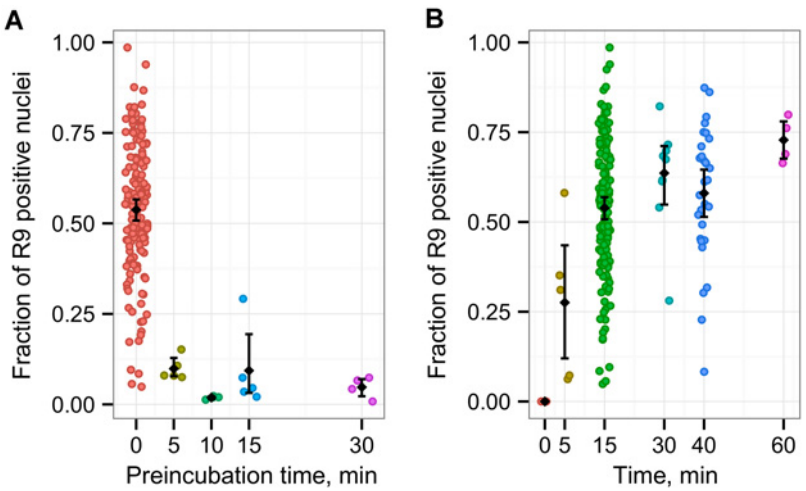

Figure 2 Dependence of R_9-TAMRA entry into the cytosol and nucleus on the duration of the pre-incubation at 15 °C before peptide addition and on the duration of the incubation with peptide

(**A**) Pre-incubation of cells at 15 °C before peptide addition inhibits R_9-TAMRA entry into the cytosol and nucleus. After addition of 2 μM R_9-TAMRA, cells were incubated for 15 min at 15 °C before washing and imaging. (**B**) Dependence of TDE on time of incubation with the peptide. After addition of 2 μM R_9-TAMRA, cells were further incubated for different times at 15 °C. Results of all individual experiments are shown as dots. Means for experiments together with 95 % confidence intervals are denoted by points with error bars.

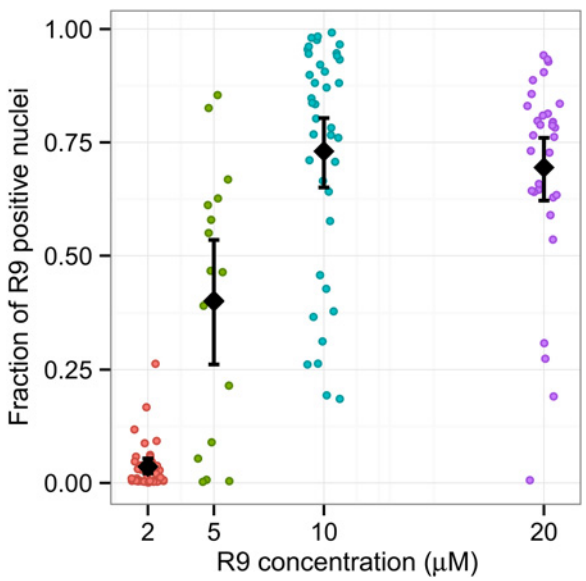

Figure 3 High peptide concentrations induce efficient entry of R_9-TAMRA into the cytosol and nucleus at 37 °C

After addition of R_9-TAMRA at different concentrations, cells were incubated for 30 min at 37 °C before washing and imaging. Results of all individual experiments are shown as dots. Means for experiments together with 95 % confidence intervals are denoted by points with error bars.

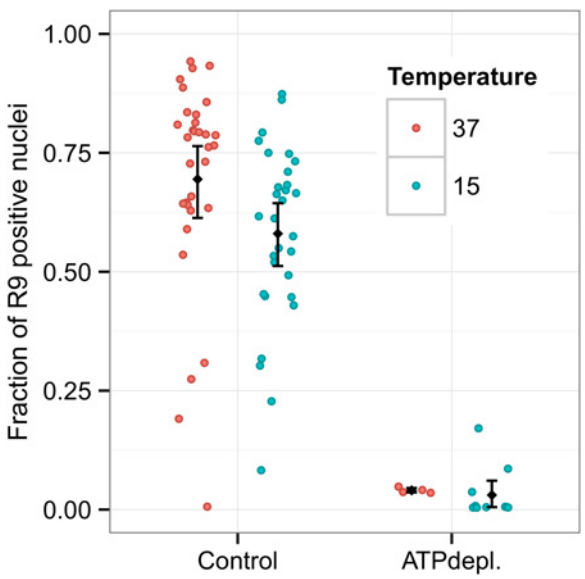

Figure 4 Both TDE and HCE are inhibited by ATP depletion

ATP-depleted or control cells were transferred into 15 °C buffer with 2 μM R_9-TAMRA or into 37 °C buffer with 20 μM R_9-TAMRA in both cases supplemented with 10 mM NaN_3 and 10 mM 2-deoxy-D-glucose and incubated for 40 or 15 min respectively, before washing and imaging. Results of all individual experiments are shown as dots. Means for experiments together with 95 % confidence intervals are denoted by points with error bars.

at high concentrations of arginine-rich CPPs at 37 °C [16]. In agreement with this study, we observed an increase in the fraction of cells with bright cytosol and nuclear staining as we incubated cells at 37 °C in the presence of R_9-TAMRA at concentrations increasing from 2 to 20 μM (Figure 3). Since entry of arginine-rich CPPs into the cytosol and nucleus at high peptide concentrations has been shown to be independent of endocytosis [17] and limited to small cargo sizes [20,26,27], we explored the TDE of R_9 conjugates with cargos of different sizes. We tested three different cargo conjugates: R_9C(PEG2000)-TAMRA (4 kDa), R_9(lysozyme)-TAMRA (16 kDa) and R_9(BSA)-TAMRA (66 kDa). In contrast with the free peptide, none of the conjugates entered the cytosol and nucleus at 2 μM concentration after the temperature drop to 15 °C (Figure 1D). Although we did not observe TDE of R_9C(PEG2000)-TAMRA at concentrations up to 10 μM (results not shown), further experiments will be required to test whether, similar to HCE, temperature drops can induce entry of R_9 conjugated to small bioactive peptides. To conclude, our data indicate that, as with the HCE pathway, efficient peptide entry induced by the temperature drop is limited to fluorescent-dye-labelled peptide.

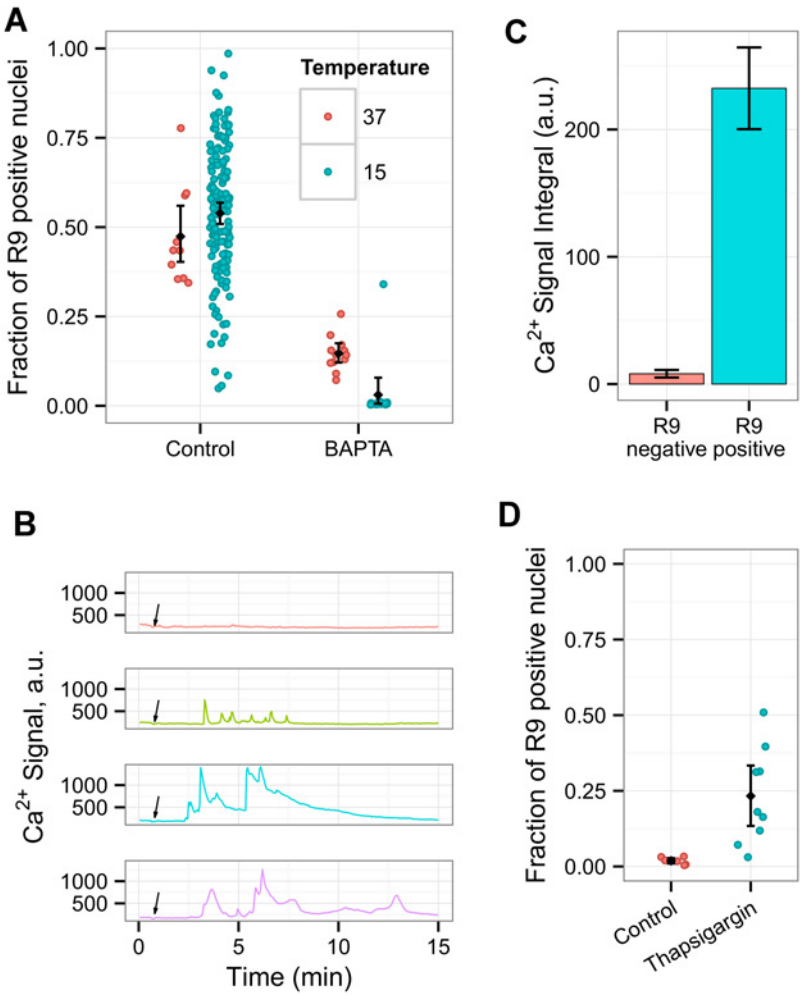

Figure 5 Both TDE and HCE depend on an increase in intracellular calcium concentration

(**A**) BAPTA-pre-loaded or control cells were transferred into 15 °C buffer containing 2 μM R_9-TAMRA or 37 °C buffer containing 20 μM R_9-TAMRA and incubated for 15 and 30 min respectively, before washing and imaging. (**B**) Four representative fluorescence signal time traces from individual cells pre-loaded with calcium indicator dye are shown. Traces are shifted vertically for clarity. Cells were imaged live at 37 °C and 20 μM R_9-TAMRA was added approximately 30 s after the start of the imaging (shown by black arrows). (**C**) Total calcium dye signal measured as an integral under the time trace from R_9-positive cells is significantly higher than that from R_9-negative cells. Cells were treated and imaged as for (**A**). Means and 95 % confidence intervals are shown. (**D**) Acute release of calcium from endoplasmic reticulum following addition of 200 nM thapsigargin together with the peptide promotes entry of R_9-TAMRA at 25 °C. Cells were incubated with the peptide for 15 min before washing and imaging. Results of all individual experiments are shown as dots. Means for experiments together with 95 % confidence intervals are denoted by points with error bars.

Depletion of intracellular ATP inhibits both TDE and HCE

Since most metabolic reactions are strongly inhibited at sub-physiological temperatures, observation of a process at low temperatures is often interpreted as an indication of energy-independence [17,19]. We evaluated the effect of ATP depletion on TDE and HCE and found that depletion of the cellular ATP pool resulting from a 30-min pre-incubation with 10 mM NaN_3 almost completely abolished both TDE and HCE (Figure 4).

TDE and HCE involve a rise in intracellular calcium

Next, we tested whether TDE and HCE depend on intracellular signalling pathways. We found that buffering of free intracellular calcium by loading the cells with 2 μM BAPTA/AM decreased the fractions of cell nuclei containing R_9-TAMRA both at 15 °C and at 37 °C (Figure 5A and Supplementary Video S1). To further study the role of intracellular calcium in the entry of R_9-TAMRA, we loaded cells with the calcium indicator Cal-520 and followed changes in intracellular calcium upon addition of the peptide at different concentrations. Whereas no changes in Cal-520 fluorescence were detectable upon addition of 2 μM R_9-TAMRA (Supplementary Video S2, left panel), application of 10 μM R_9-TAMRA induced multiple spikes of intracellular calcium in some of the cells (Figure 5B, three bottom traces; Supplementary Video S2, right panel). Peak amplitudes of these spikes were comparable to the amplitude of increase in intracellular calcium induced by addition of 0.2 μM SERCA inhibitor thapsigargin (Supplementary Figure S3). SERCAs counterbalance passive leakage of Ca^{2+} from the endoplasmic reticulum and their inhibition leads to a transient increase in intracellular Ca^{2+} concentration [28]. Peptide-induced calcium spikes and peptide entry were correlated, with the cells showing a significant peptide entry also displaying a higher total integrated calcium dye signal than the cells with no nuclear peptide staining (Figure 5C).

We reasoned that if blocking calcium spikes inhibits peptide entry, an increase in cytosol calcium could promote entry. Indeed, we induced peptide entry into a significant fraction of the

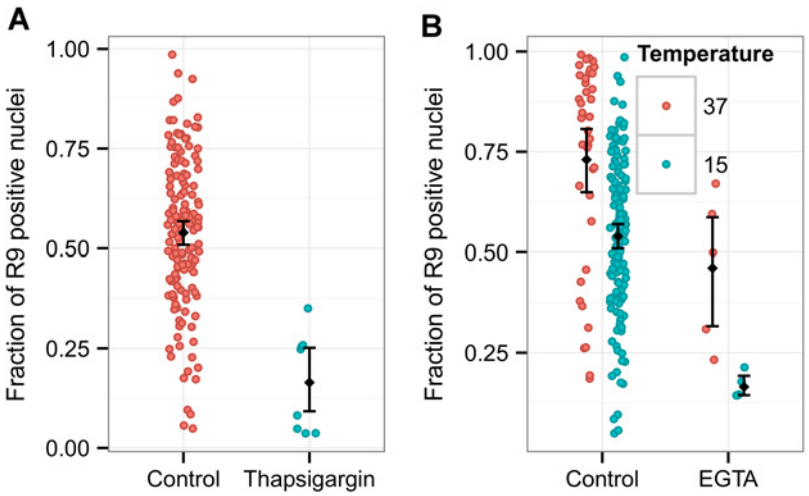

Figure 6 Both intracellular calcium stores and extracellular calcium are needed for efficient entry of R_9-TAMRA into the cytosol and nucleus

(**A**) Control cells or cells pre-incubated with 2 μM thapsigargin for 30 min were incubated with 2 μM R_9-TAMRA at 15 °C for 15 min before washing and imaging. (**B**) Cells were incubated for 15 min with 2 μM R_9-TAMRA at 15 °C or with 20 μM R_9-TAMRA at 37 °C in HMEM or in calcium-free buffer supplemented with 1 mM EGTA. Results of all individual experiments are shown as dots. Means for experiments together with 95 % confidence intervals are denoted by points with error bars.

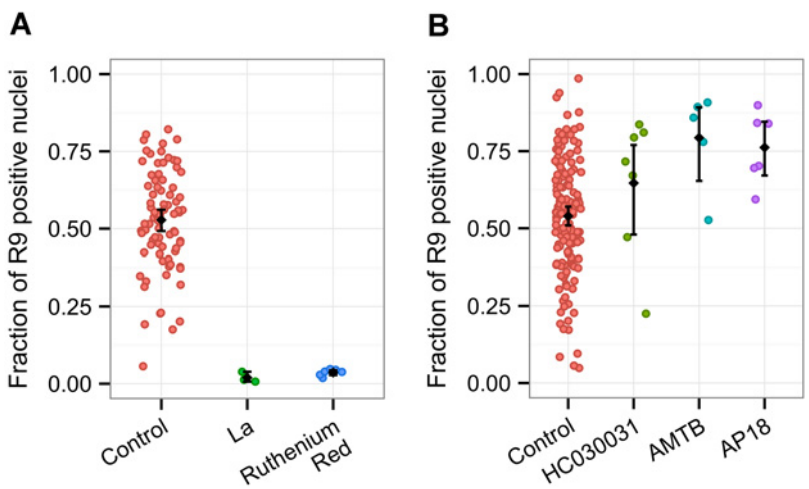

Figure 7 Non-specific cation channel antagonists but not specific cold-sensitive TRP channels antagonists inhibit TDE

(**A**) After addition of 2 μM R_9-TAMRA with La^{3+} (100 μM) or Ruthenium Red (100 μM) or without an inhibitor (control), the cells were incubated for 15 min at 15 °C before washing and imaging. (**B**) Specific inhibitors of TRPA1 and TRPM8 cold-sensitive channels, HC030031 (100 μM), AP18 (100 μM) and AMTB (100 μM), were added together with the peptide without pre-incubation. After addition of the peptide with or without the drug, the cells were incubated for 15 min at 15 °C before washing and imaging. Results of all individual experiments are shown as dots. Means for experiments together with 95 % confidence intervals are denoted by points with error bars.

cells at 25 °C by adding 0.2 μM SERCA inhibitor thapsigargin simultaneously with the CPP application (Figure 5D). These results suggest that a rise in intracellular calcium is an important step in increasing the permeability of plasma membrane to R_9-TAMRA.

Both decrease in extracellular calcium concentration and depletion of calcium from intracellular stores inhibit TDE and HCE

To clarify the role of intracellular calcium stores in R_9-TAMRA entry, we depleted the endoplasmic reticulum store by pre-incubating the cells with 2 μM thapsigargin for 40 min. This led to a significant inhibition of low-temperature-induced peptide entry (Figure 6A), suggesting that TDE depends on calcium release from the endoplasmic reticulum. On the other hand, addition of the peptide to cells in calcium-free medium inhibited its entry both at 15 °C and at 37 °C (Figure 6B), suggesting that the activation of the TDE and HCE pathways also depends on extracellular calcium.

Non-selective cation channel inhibitors suppress TDE, whereas specific inhibitors of temperature-sensitive TRP channels do not

Dependence on extracellular calcium suggests possible involvement of plasma membrane calcium channels in the induction of R_9-TAMRA entry. Indeed, we observed a significant decrease in the fraction of R_9-TAMRA-positive cells in the presence of the non-selective cation channel inhibitors La^{3+} and ruthenium red (Figure 7A). Since members of the TRP family of non-selective cation channels, namely TRPA1 and TRPM8,

have been implicated in cold sensing *in vivo* and demonstrate a cold-activated current response *in vitro* [29,30], we assessed their involvement in cold-induced R_9-TAMRA entry. Neither specific antagonists of TRPA1 HC030031 and AP18 nor specific antagonists of TRPM8 channel AMTB inhibited cold-induced entry of R_9-TAMRA (Figure 7B). Thus, our data provide support for the involvement of cation channels in the activation of peptide entry pathways, whereas the identities of the calcium channels involved remain to be clarified.

TDE and HCE depend on the cell-surface exposure of phosphatidylserine

Intracellular calcium is a ubiquitous second messenger and affects a vast array of different processes inside the cell including those controlling trans-bilayer lipid asymmetry of the plasma membrane. An increase in calcium concentration induces redistribution of PS, which normally resides only in the inner leaflet of the plasma membrane, into the outer leaflet [23,24]. We found that blocking accessible PS with the PS-binding protein LactC2 strongly inhibited both TDE and HCE (Figure 8), suggesting the importance of PS exposure in peptide entry. We also evaluated the effects of inhibitors of acid sphingomyelinase that have been implicated in HCE, through formation of ceramide on the plasma membrane [20,31]. Neither chlorpromazine nor nortriptyline had an effect on TDE, whereas imipramine had only a modest inhibitory effect (Figure 9).

Increase in intracellular calcium concentration induces efficient entry of R_9 into the cytosol and nucleus

Mechanistic dependence of the R9 entry on calcium signalling suggested that drugs known to release calcium from intracellular stores may lower concentration of the R_9-TAMRA required for its efficient entry at 37°C. We treated the cells with flufenamic acid, a member of fenamate class of non-steroidal anti-inflammatory drugs, which have been shown to release calcium form mitochondria [32,33]. Since, in our experiments, we consistently observed a several minute delay between addition of 10 μM R_9-TAMRA and the onset of calcium spikes (Figure 5B; Supplementary Video S2), we applied flufenamic acid to cells either together with 2 μM R_9-TAMRA or 5 min after the peptide addition. We observed no effect on the entry of R_9-TAMRA when flufenamic acid was added together with the peptide (Figure 10A). In contrast, application of flufenamic acid 5 min after peptide addition resulted in efficient entry of R_9-TAMRA into the cytosol and nucleus of many cells (Figure 10A). Interestingly, flufenamic acid applied either with or before the peptide induced an increase in intracellular calcium concentration (Figure 10B). However, whereas addition of drug 5 min after peptide application resulted in a sustained increase in calcium concentration (Figure 10B, top trace), in the case of simultaneous application of flufenamic acid and the peptide, the calcium level rapidly returned to background levels (Figure 10B, bottom trace). We conclude that efficient entry of R_9-TAMRA can be promoted by a drug-induced increase in intracellular calcium concentration.

DISCUSSION

Despite considerable interest in arginine-rich CPPs as potential drug-delivery vehicles, the mechanism of their entry into cells remains controversial and poorly understood. In the present paper, we report that a rapid decrease in temperature induces very efficient entry of R_9-TAMRA into the cytosol and nucleus

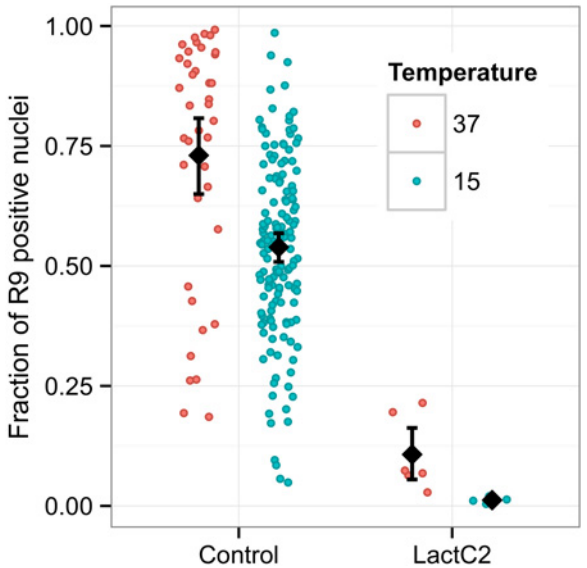

Figure 8 PS-binding LactC2 strongly inhibits both TDE and HCE

Cells were incubated for 15 min with 2 μM R_9-TAMRA at 15°C or with 20 μM R_9-TAMRA at 37°C in a buffer supplemented or not with LactC2 at 100 μg/ml. Results of all individual experiments are shown as dots. Means for experiments together with 95% confidence intervals are denoted by points with error bars.

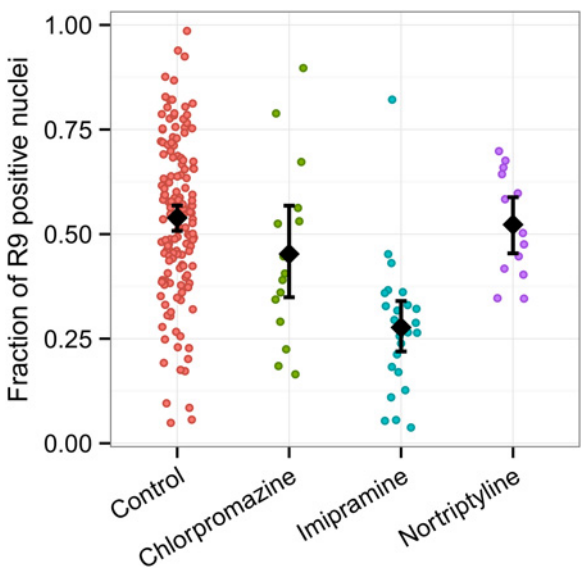

Figure 9 Inhibitors of acid sphingomyelinase do not inhibit TDE

Cells were pre-incubated with imipramine (10 μM), nortriptyline (10 μM) or chlorpromazine (10 μg/ml) or kept without any drug for 30 min at 37°C. Drugs at the same concentrations were also present during incubation with the peptide. After addition of 2 μM R_9-TAMRA with or without drugs, the cells were incubated for 15 min at 15°C before washing and imaging. Results of all individual experiments are shown as dots. Means for experiments together with 95% confidence intervals are denoted by points with error bars.

of adherent HeLa cells at 2 μM peptide concentrations. At physiological temperature, entry of the peptide into the cytosol and nucleus is observed only at higher peptide concentrations ($\geqslant$10 μM). Low-temperature-induced entry of arginine-rich CPPs into the cytosol and nucleus has been previously reported for several suspension cell lines [34,35]. However, in apparent contradiction to our results, in adherent cell lines, including the HeLa cell line used in the present study, entry of the CPP into the cytosol and nucleus in these studies was observed only at

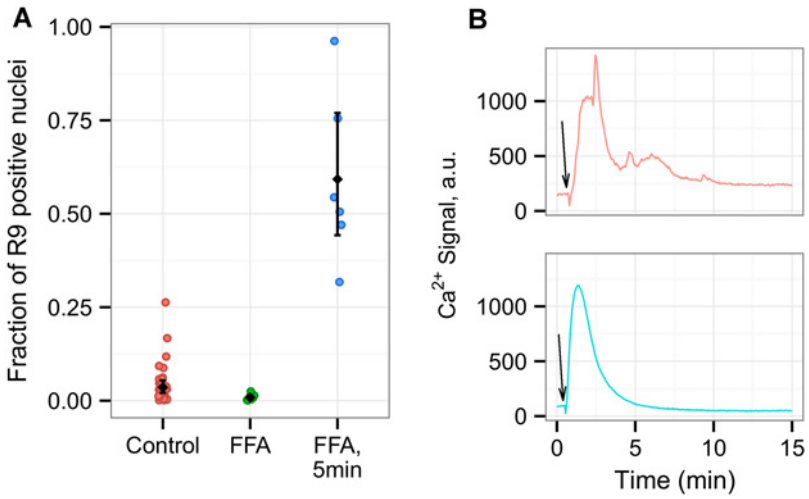

Figure 10 An increase in intracellular calcium concentration by flufenamic acid induces efficient entry of R_9-TAMRA into the cytosol and nucleus at 37 °C

(**A**) Cells were transferred into 37 °C buffer containing 2 μM R_9-TAMRA. Flufenamic acid (100 μM) was added either together with the peptide (NEFA) or 5 min later (NEFA, 5 min) and drug was not added to control cells (control). In all cases, cells were incubated for 15 min in the presence of the peptide before washing and imaging. Results of all individual experiments are shown as dots. Means for experiments together with 95 % confidence intervals are denoted by points with error bars. (**B**) Representative fluorescence signal time traces from individual cells pre-loaded with calcium indicator dye are shown. Traces are shifted vertically for clarity. Cells were imaged live at 37 °C and 100 μM flufenamic acid was added approximately 30 s after the start of the imaging (shown by black arrows). R_9-TAMRA (2 μM) was added together with the flufenamic acid (bottom trace) or 5 min before application of the drug.

significantly higher peptide concentrations ($\geqslant$20 μM) [34]. This discrepancy is probably due to the transient nature of TDE in HeLa cells. Both TDE and HCE are observed only in a sub-population of cells and are limited to fluorescent-dye-labelled peptide. The efficiency of TDE and HCE pathways is striking; we estimate, on the basis of the intensity of the fluorescence signal that the amount of the peptide entering an individual cell at 15 °C within 15 min is at least 50-fold higher than the amount of the peptide entering a cell within 40 min at 37 °C by endocytosis. Importantly, such efficient entry is limited to the cationic peptide and is not accompanied by the entry of concomitantly added small membrane-impermeant dyes such as calcein or SYTOX Green.

Both TDE and HCE were strongly inhibited by ATP depletion. Since most metabolic processes are inhibited at sub-physiological temperatures, such energy-dependence at 15 °C is unusual, but not unique and is well established for maintaining lipid asymmetry of plasma membrane by aminotranslocase [36,37]. It is not clear at the moment whether ATP hydrolysis is required for actual transport of the peptide across the plasma membrane or for upstream processes that activate the entry pathway.

We also observed an intriguing dependence of R_9-TAMRA entry on the rise in intracellular Ca^{2+} concentration. Increase in intracellular Ca^{2+} concentration was previously observed for several amphipathic CPPs and has been attributed to membrane disordering during peptide entry [38]. Lorents et al. [38] did not observe an increase in intracellular Ca^{2+} concentration in the presence of unconjugated R_9 peptide, in contrast with our results with both R_9-TAMRA (Figures 5B and 5C; Supplementary Video S2) and unconjugated peptide (not shown). One possible explanation for this discrepancy is that the changes in Ca^{2+} concentration that we observed in the present study are transient and were detectable only by means of relatively fast time-lapse imaging, whereas end-point measurements were used by Lorents et al. [38]. Inhibition of TDE and HCE by BAPTA/AM indicates that increase in intracellular Ca^{2+} concentration precedes peptide entry and suggests that TDE and HCE are multistep processes involving intracellular signalling pathways. What is the mechanism of the R_9-TAMRA-induced increase in Ca^{2+} concentration? One possibility is that cell-surface-bound R_9-TAMRA modulates activity of plasma membrane cation channels. Indeed, we have previously reported that R_9-TAMRA strongly modulates conductance of the gramicidin A channel reconstituted into black lipid membranes [11]. Alternatively, interaction of the peptide with cell-surface receptors may lead to their activation and to the opening of associated Ca^{2+} channels. In either case, the inhibition of peptide entry by non-specific cation channel blockers supports involvement of cation channels on the plasma membrane in TDE. Interestingly, we observed a significant variation in cell response to the peptide, with high peptide concentrations inducing repetitive spikes of intracellular Ca^{2+} in some but not all cells within the same observation field. Such variable signalling response to different stimuli has been observed for a broad range of cell types [39–41]. The nature of this variability remains to be explored, but it is likely to be responsible for variability in peptide entry given that the appearance of calcium spikes and peptide entry were strongly correlated. We also demonstrated that increasing intracellular calcium with flulfenamic acid induces entry of 2 μM R_9-TAMRA at 37 °C, suggesting that manipulation of intracellular calcium levels could be used to promote peptide entry at physiological temperatures.

The mechanism of temperature sensing in TDE activation also remains unclear. Given the importance of extracellular calcium entry and involvement of cation channels it is possible that promotion of the entry by low temperature is dependent on cold-activated non-selective cation channels. However, our data do not support the involvement of TRPA1 and TRPM8 channels, which play a major role in the increase in intracellular Ca^{2+} in cold sensation [29,30,42]. The roles of other cation channels implicated in the cold response, such as TREK1 and TRAAK [29,30] and the roles of other possible mechanisms of cold activation remains to be explored. For example, the physical state of membrane bilayer might play a role in TDE activation, given that liquid-ordered/liquid-disordered phase separation has been observed in giant vesicles derived from plasma membrane over a temperature range of 10–30 °C [43].

The steps downstream of the rise in intracellular calcium that lead to peptide entry remain elusive. Brock and colleagues [20] have shown the importance of acid sphingomyelinase-dependent formation of ceramide on the plasma membrane in the HCE of arginine-rich CPPs. Independently, Futaki and colleagues [19] demonstrated cell-surface exposure of PS upon incubation of cells with high concentrations of oligo-arginines. In the present study, we inhibited both TDE and HCE by adding LactC2, implicating exposure of PS on the cell surface in the process. However, we observed no effect of acid sphingomyelinase inhibitors on peptide entry at low temperature.

To conclude, we describe in the present paper a highly efficient intracellular calcium-regulated pathway of oligo-arginine entry into the cytosol and nucleus of adherent cells. Like the HCE pathway, the TDE pathway is limited to fluorescent-dye-labelled peptide and could be useful for delivery of low-molecular-mass drugs such as small bioactive peptides. We expect further study of this phenomenon to provide new insights into transport processes on plasma membrane and to yield better approaches for intracellular delivery of at least small drugs *in vivo*.

AUTHOR CONTRIBUTION

Kamran Melikov, Ann Hara and Kwabena Yamoah performed most of the experimental work and data analysis. Elena Zaitseva and Eugene Zaitsev purified and characterized LactC2. Kamran Melikov and Leonid Chernomordik designed the research and wrote the paper. All the authors read and agreed on the final version of the paper.

ACKNOWLEDGEMENT

We thank Sergei Pourmal for his help with some of the experiments at the onset of the project.

FUNDING

This work was supported by the Intramural Research Program of the Eunice Kennedy Shriver National Institute of Child Health and Human Development, National Institutes of Health (to L.V.C.).

REFERENCES

1 van den Berg, A. and Dowdy, S.F. (2011) Protein transduction domain delivery of therapeutic macromolecules. Curr. Opin. Biotechnol. **22**, 888–893 CrossRef PubMed
2 Nakase, I., Akita, H., Kogure, K., Gräslund, A., Langel, U., Harashima, H. and Futaki, S. (2012) Efficient intracellular delivery of nucleic acid pharmaceuticals using cell-penetrating peptides. Acc. Chem. Res. **45**, 1132–1139 CrossRef PubMed
3 Margus, H., Padari, K. and Pooga, M. (2012) Cell-penetrating peptides as versatile vehicles for oligonucleotide delivery. Mol. Ther. **20**, 525–533 CrossRef PubMed
4 Melikov, K. and Chernomordik, L.V. (2005) Arginine-rich cell penetrating peptides: from endosomal uptake to nuclear delivery. Cell. Mol. Life Sci. **62**, 2739–2749 CrossRef PubMed
5 Edenhofer, F. (2008) Protein transduction revisited: novel insights into the mechanism underlying intracellular delivery of proteins. Curr. Pharm. Des. **14**, 3628–3636 CrossRef PubMed
6 Erazo-Oliveras, A., Muthukrishnan, N., Baker, R., Wang, T.-Y. and Pellois, J.-P. (2012) Improving the endosomal escape of cell-penetrating peptides and their cargos: strategies and challenges. Pharmaceuticals **5**, 1177–1209 CrossRef PubMed
7 Mäger, I., Eiríksdóttir, E., Langel, K., El Andaloussi, S. and Langel, Ü. (2010) Assessing the uptake kinetics and internalization mechanisms of cell-penetrating peptides using a quenched fluorescence assay. Biochim. Biophys. Acta **1798**, 338–343 CrossRef PubMed
8 Madani, F., Abdo, R., Lindberg, S., Hirose, H., Futaki, S., Langel, Ü. and Gräslund, A. (2013) Modeling the endosomal escape of cell-penetrating peptides using a transmembrane pH gradient. Biochim. Biophys. Acta **1828**, 1198–1204 CrossRef PubMed
9 Björklund, J., Biverståhl, H., Gräslund, A., Mäler, L. and Brzezinski, P. (2006) Real-time transmembrane translocation of penetratin driven by light-generated proton pumping. Biophys. J. **91**, L29–L31 CrossRef PubMed
10 Yang, S.-T., Zaitseva, E., Chernomordik, L.V. and Melikov, K. (2010) Cell-penetrating peptide induces leaky fusion of liposomes containing late endosome-specific anionic lipid. Biophys. J. **99**, 2525–2533 CrossRef PubMed
11 Gurnev, P.A., Yang, S.-T., Melikov, K.C., Chernomordik, L.V. and Bezrukov, S.M. (2013) Cationic cell-penetrating peptide binds to planar lipid bilayers containing negatively charged lipids but does not induce conductive pores. Biophys. J. **104**, 1933–1939 CrossRef PubMed
12 Abes, R., Moulton, H.M., Clair, P., Yang, S.-T., Abes, S., Melikov, K., Prevot, P., Youngblood, D.S., Iversen, P.L., Chernomordik, L.V. et al. (2008) Delivery of steric block morpholino oligomers by (R-X-R)4 peptides: structure-activity studies. Nucleic Acids Res. **36**, 6343–6354 CrossRef PubMed
13 Wadia, J.S., Stan, R.V. and Dowdy, S.F. (2004) Transducible TAT-HA fusogenic peptide enhances escape of TAT-fusion proteins after lipid raft macropinocytosis. Nat. Med. **10**, 310–315 CrossRef PubMed
14 Duchardt, F., Fotin-Mleczek, M., Schwarz, H., Fischer, R. and Brock, R. (2007) A comprehensive model for the cellular uptake of cationic cell-penetrating peptides. Traffic **8**, 848–866 CrossRef PubMed
15 Ziegler, A., Nervi, P., Dürrenberger, M. and Seelig, J. (2005) The cationic cell-penetrating peptide CPP(TAT) derived from the HIV-1 protein TAT is rapidly transported into living fibroblasts: optical, biophysical and metabolic evidence. Biochemistry **44**, 138–148 CrossRef PubMed
16 Tünnemann, G., Ter-Avetisyan, G., Martin, R.M., Stöckl, M., Herrmann, A. and Cardoso, M.C. (2008) Live-cell analysis of cell penetration ability and toxicity of oligo-arginines. J. Pept. Sci. **14**, 469–476 CrossRef PubMed
17 Ter-Avetisyan, G., Tunnemann, G., Nowak, D., Nitschke, M., Herrmann, A., Drab, M. and Cardoso, M.C. (2009) Cell entry of arginine-rich peptides is independent of endocytosis. J. Biol. Chem. **284**, 3370–3378 CrossRef PubMed
18 Kosuge, M., Takeuchi, T., Nakase, I., Jones, A.T. and Futaki, S. (2008) Cellular Internalization and distribution of arginine-rich peptides as a function of extracellular peptide concentration, serum, and plasma membrane associated proteoglycans. Bioconjug. Chem. **19**, 656–664 CrossRef PubMed
19 Hirose, H., Takeuchi, T., Osakada, H., Pujals, S., Katayama, S., Nakase, I., Kobayashi, S., Haraguchi, T. and Futaki, S. (2012) Transient focal membrane deformation induced by arginine-rich peptides leads to their direct penetration into cells. Mol. Ther. **20**, 984–993 CrossRef PubMed
20 Verdurmen, W.P. R., Thanos, M., Ruttekolk, I.R., Gulbins, E. and Brock, R. (2010) Cationic cell-penetrating peptides induce ceramide formation via acid sphingomyelinase: Implications for uptake. J. Control. Release **147**, 171–179 CrossRef PubMed
21 Andersen, M.H., Graversen, H., Fedosov, S.N., Petersen, T.E. and Rasmussen, J.T. (2000) Functional analyses of two cellular binding domains of bovine lactadherin. Biochemistry **39**, 6200–6206 CrossRef PubMed
22 Otzen, D.E., Blans, K., Wang, H., Gilbert, G.E. and Rasmussen, J.T. (2012) Lactadherin binds to phosphatidylserine-containing vesicles in a two-step mechanism sensitive to vesicle size and composition. Biochim. Biophys. Acta **1818**, 1019–1027 CrossRef PubMed
23 Leventis, P.A. and Grinstein, S. (2010) The distribution and function of phosphatidylserine in cellular membranes. Annu. Rev. Biophys. **39**, 407–427 CrossRef PubMed
24 Bevers, E.M. and Williamson, P.L. (2010) Phospholipid scramblase: an update. FEBS Lett. **584**, 2724–2730 CrossRef PubMed
25 Shao, C., Novakovic, V.A., Head, J.F., Seaton, B.A. and Gilbert, G.E. (2008) Crystal structure of lactadherin C2 domain at 1.7Å resolution with mutational and computational analyses of its membrane-binding motif. J. Biol. Chem. **283**, 7230–7241 CrossRef PubMed
26 Maiolo, J.R., Ferrer, M. and Ottinger, E.A. (2005) Effects of cargo molecules on the cellular uptake of arginine-rich cell-penetrating peptides. Biochim. Biophys. Acta **1712**, 161–172 CrossRef PubMed
27 Tunnemann, G., Martin, R.M., Haupt, S., Patsch, C., Edenhofer, F. and Cardoso, M.C. (2006) Cargo-dependent mode of uptake and bioavailability of TAT-containing proteins and peptides in living cells. FASEB J. **20**, 1775–1784 CrossRef PubMed
28 Treiman, M., Caspersen, C. and Christensen, S.B. (1998) A tool coming of age: thapsigargin as an inhibitor of sarco-endoplasmic reticulum Ca^{2+}-ATPases. Trends Pharmacol. Sci. **19**, 131–135 CrossRef PubMed
29 Babes, A. (2009) Ion channels involved in cold detection in mammals: TRP and non-TRP mechanisms. Biophys. Rev. **1**, 193–200 CrossRef
30 McKemy, D.D. (2013) The molecular and cellular basis of cold sensation. ACS Chem. Neurosci. **4**, 238–247 CrossRef PubMed

31 Kornhuber, J., Tripal, P., Reichel, M., Terfloth, L., Bleich, S., Wiltfang, J. and Gulbins, E. (2008) Identification of new functional inhibitors of acid sphingomyelinase using a structure – property – activity relation model. J. Med. Chem. **51**, 219–237 CrossRef PubMed

32 Poronnik, P., Ward, M.C. and Cook, D.I. (1992) Intracellular Ca^{2+} release by flufenamic acid and other blockers of the non-selective cation channel. FEBS Lett. **296**, 245–248 CrossRef PubMed

33 Chi, Y., Li, K., Yan, Q., Koizumi, S., Shi, L., Takahashi, S., Zhu, Y., Matsue, H., Takeda, M., Kitamura, M. et al. (2011) Nonsteroidal anti-inflammatory drug flufenamic acid is a potent activator of amp-activated protein kinase. J. Pharmacol. Exp. Ther. **339**, 257–266 CrossRef PubMed

34 Watkins, C.L., Schmaljohann, D., Futaki, S. and Jones, A.T. (2009) Low concentration thresholds of plasma membranes for rapid energy-independent translocation of a cell-penetrating peptide. Biochem. J. **420**, 179–189 CrossRef PubMed

35 Fretz, M.M., Penning, N.A., Al-Taei, S., Futaki, S., Takeuchi, T., Nakase, I., Storm, G. and Jones, A.T. (2007) Temperature-, concentration- and cholesterol-dependent translocation of L- and D-octa-arginine across the plasma and nuclear membrane of CD34 + leukaemia cells. Biochem. J. **403**, 335–342 CrossRef PubMed

36 Martin, O.C. and Pagano, R.E. (1987) Transbilayer movement of fluorescent analogs of phosphatidylserine and phosphatidylethanolamine at the plasma membrane of cultured cells. Evidence for a protein-mediated and ATP-dependent process(es). J. Biol. Chem. **262**, 5890–5898 PubMed

37 Kay, J.G., Koivusalo, M., Ma, X., Wohland, T. and Grinstein, S. (2012) Phosphatidylserine dynamics in cellular membranes. Mol. Biol. Cell **23**, 2198–2212 CrossRef PubMed

38 Lorents, A., Kodavali, P.K., Oskolkov, N., Langel, Ü., Hällbrink, M. and Pooga, M. (2012) Cell-penetrating peptides split into two groups based on modulation of intracellular calcium concentration. J. Biol. Chem. **287**, 16880–16889 CrossRef PubMed

39 Bao, X.R., Fraser, I.D.C., Wall, E.A., Quake, S.R. and Simon, M.I. (2010) Variability in G-protein-coupled signaling studied with microfluidic devices. Biophys. J. **99**, 2414–2422 CrossRef PubMed

40 Appleby, P.A., Shabir, S., Southgate, J. and Walker, D. (2015) Sources of variability in cytosolic calcium transients triggered by stimulation of homogeneous uro-epithelial cell monolayers. J.R. Soc. Interface **12**, 20141403 CrossRef PubMed

41 Arrol, H.P., Church, L.D., Bacon, P.A. and Young, S.P. (2008) Intracellular calcium signalling patterns reflect the differentiation status of human T cells. Clin. Exp. Immunol. **153**, 86–95 CrossRef PubMed

42 Latorre, R., Brauchi, S., Madrid, R. and Orio, P. (2011) A cool channel in cold transduction. Physiology **26**, 273–285 CrossRef PubMed

43 Johnson, S.A., Stinson, B.M., Go, M.S., Carmona, L.M., Reminick, J.I., Fang, X. and Baumgart, T. (2010) Temperature-dependent phase behavior and protein partitioning in giant plasma membrane vesicles. Biochim. Biophys. Acta **1798**, 1427–1435 CrossRef PubMed

Received 2 March 2015/11 August 2015; accepted 13 August 2015
Accepted Manuscript online 13 August 2015, doi:10.1042/BJ20150272